



# Negative Photoconductive Effects in Uncooled InAs Nanowire Photodetectors

Xingfei Zhang<sup>1,2</sup>, Yiyun Zhang<sup>1,2\*</sup>, Dong Pan<sup>2,3\*</sup>, Xiaoyan Yi<sup>1,2</sup>, Jianhua Zhao<sup>2,3</sup> and Jinmin Li<sup>1,2</sup>

<sup>1</sup>R&D Center for Solid-state Lighting, Institute of Semiconductors, Chinese Academy of Sciences, Beijing, China, <sup>2</sup>State Key Laboratory of Superlattices and Microstructures, Institute of Semiconductors, Chinese Academy of Sciences, Beijing, China, <sup>3</sup>Center of Materials Science and Optoelectronics Engineering, University of Chinese Academy of Sciences, Beijing, China

One-dimensional, direct, and narrow band gap indium arsenide (InAs) nanowires (NWs) have been emerging with great potentials for the next-generation wide-spectrum photodetectors. In this study, metal–semiconductor–metal (MSM) structure InAs NW-based photodetectors were fabricated by transferring MBE-grown NWs onto a sapphire substrate via a mechanical stamping method. These NW detectors exhibit strong negative photoconductive (NPC) effects, which are likely caused by the carrier dynamics in the “core-shell” structure of the NWs. Specifically, under the irradiation of a 405 nm violet laser, the maximum  $I_{\text{dark}}/I_{\text{light}}$  ratio reaches  $\sim 10^2$  and the NPC gain reaches  $10^5$  at a low bias voltage of 0.2 V. At room temperature, the rise and decay times of InAs NW devices are 0.005 and 2.645 s, respectively. These InAs NW devices with a high  $I_{\text{dark}}/I_{\text{light}}$  ratio and NPC gain can be potentially used in the field of vis/near-IR light communication in the future.

**Keywords:** InAs, nanowires, negative photoconductivity, photodetector, wide-spectrum

## INTRODUCTION

In recent years, III-V semiconductor nanowires (NWs) have attracted great attention in the areas of wide-spectrum photodetectors with high photoconductive gain and fast response and have achieved tremendous progress [1–10]. Among them, indium arsenide (InAs) NWs are used as an alternative material for photodetectors because of their high electron mobility, intrinsic narrow band gap (0.35 eV), and other excellent properties [11–19]. In the meanwhile, InAs NWs also have a huge specific surface area and abundant surface defect states, which makes them outstand as an important role in photosensitive devices [20–26]. Interestingly, unlike other NWs that have a positive photoconductive (PPC) effect [17, 27, 28], the intrinsic InAs NWs have negative photoconductive (NPC) effects in contrast [29–31], that is, as the excitation power intensity increases, the photocurrent in the channel would gradually decrease, some of which is even cut off [29]. The main reason is that the indium at the outermost layer of the NW is easily oxidized in the air to form indium oxide, leading to numerous defect-trapping centers with the indium oxide ( $\text{InO}_x$ ) simultaneously [30, 32]. It is often called as the photogating layer (PGL) [29]. So far, designs of most photodetectors based on NWs primarily aim to form a junction, in general, to achieve a larger net photocurrent, such as the Schottky junction [33, 34], p-n junction [17], or heterojunction [35, 36], by suppressing the dark current as much as possible. Among them, a typical design is the metal–semiconductor–metal (MSM) photodetector, which is realized by two back-to-back Schottky junctions. Recently, a new type of NW photodetector has been demonstrated to enhance the response through the ferroelectric field [37]. These detectors have extremely high

## OPEN ACCESS

### Edited by:

Jun Wang,  
University of Electronic Science and  
Technology of China, China

### Reviewed by:

Yaping Dan,  
Shanghai Jiao Tong University, China  
Saikiran Vadavalli,  
Gandhi Institute of Technology and  
Management (GITAM), India

### \*Correspondence:

Yiyun Zhang  
yyzhang@semi.ac.cn  
Dong Pan  
pandong@semi.ac.cn

### Specialty section:

This article was submitted to  
Optics and Photonics,  
a section of the journal  
Frontiers in Physics

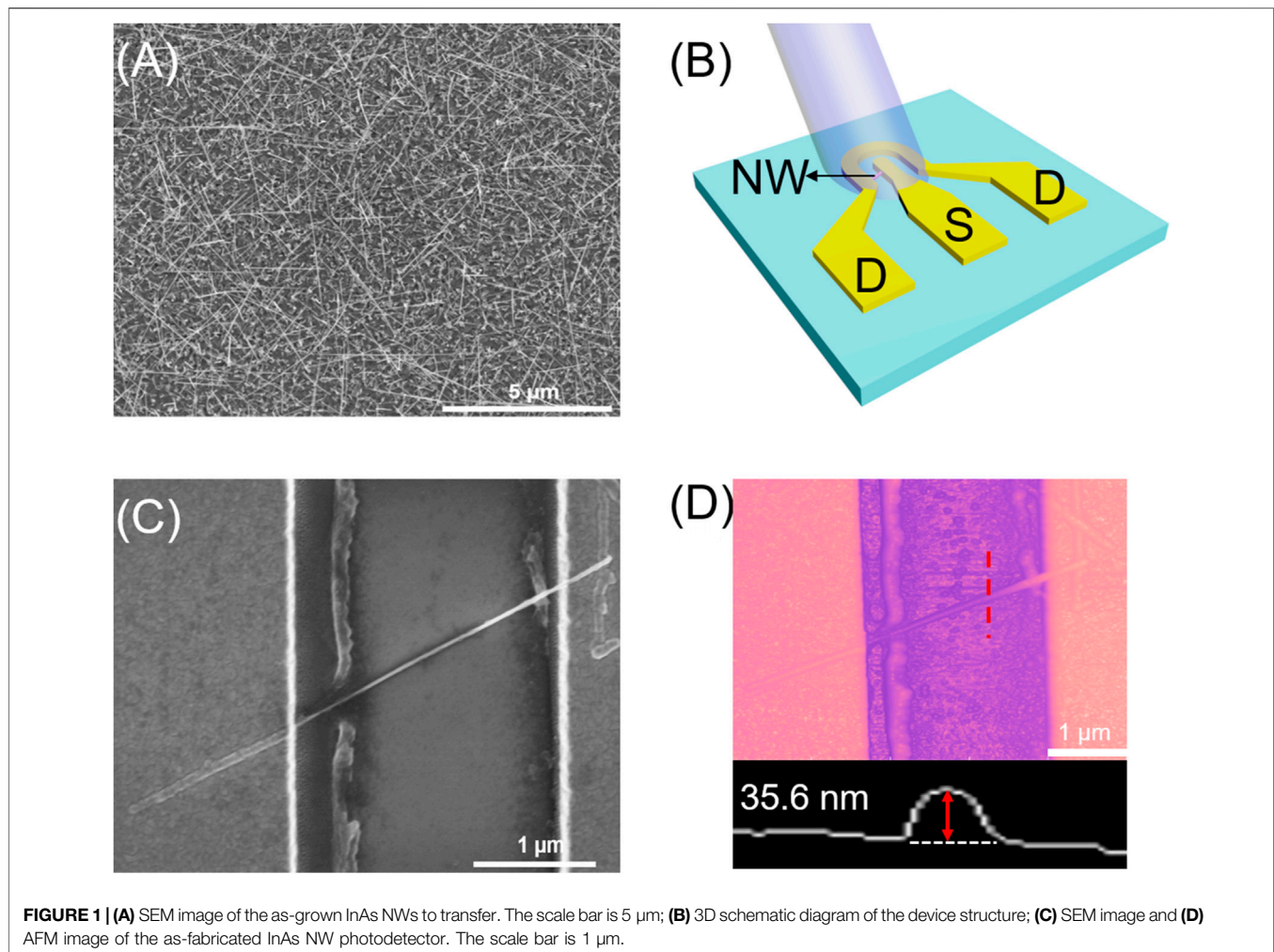
Received: 15 June 2021

Accepted: 13 September 2021

Published: 21 October 2021

### Citation:

Zhang X, Zhang Y, Pan D, Yi X, Zhao J  
and Li J (2021) Negative  
Photoconductive Effects in Uncooled  
InAs Nanowire Photodetectors.  
Front. Phys. 9:725680.  
doi: 10.3389/fphy.2021.725680



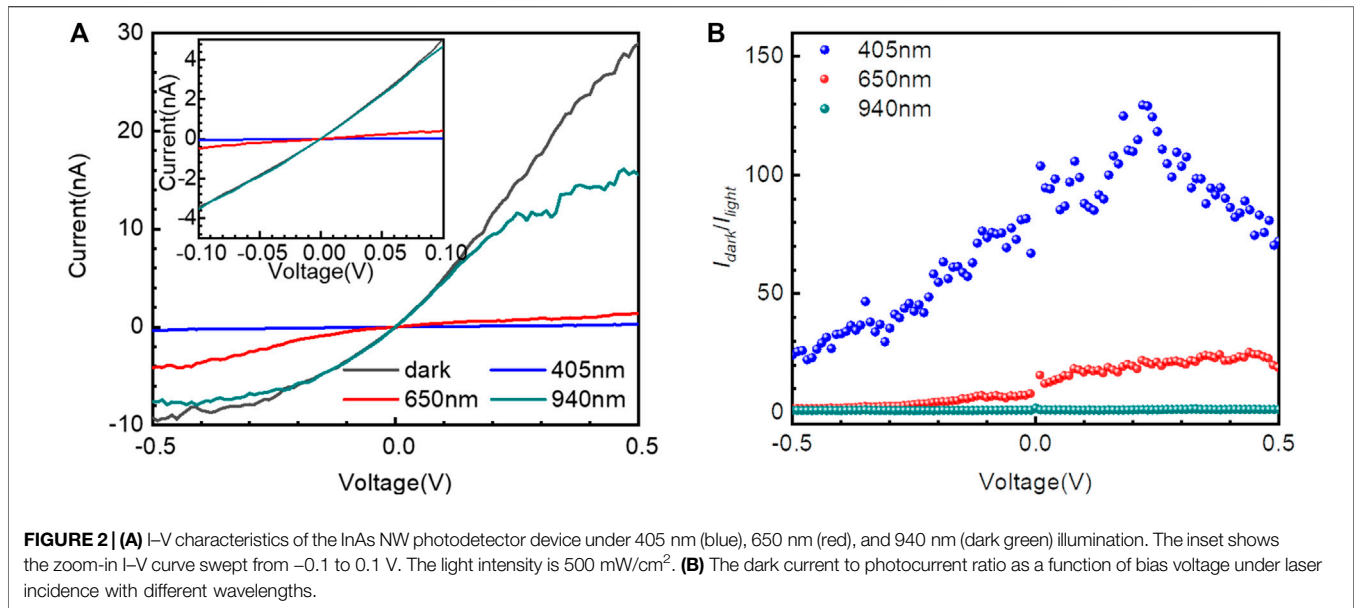
responsivity due to the low dark current. The use of narrow band gap materials readily enables wide-spectrum detection and extends their applications, but it is difficult to achieve good responsivity at all wavelengths of interest [28, 30].

In this work, to explore the possibility of using InAs NWs as the broadband photodetectors, we propose an MSM photodetector based on InAs NWs grown by MBE. The response of the device under various wavelengths of laser irradiation is investigated. A considerable NPC effect is found, which is strongly dependent on the wavelengths of incidence. It can be largely attributed to the carrier redistribution dynamics in the intrinsic “core-shell” structure, consisting of the oxides on the crust of the NW and its interiors. Especially, under 405 nm laser irradiation, the detector has the largest  $I_{dark}/I_{light}$  ratio, responsivity, and response speed.

## EXPERIMENTAL SECTION

The InAs NW array was grown on commercial *p*-type silicon (111) wafers by MBE [38]. To start the processing, InAs NWs

were first transferred onto pre-cleaned sapphire substrates via a mechanical stamping method. Then, standard photolithography and electron beam evaporation were used to fabricate the source and drain metal electrodes. A film of Ti/Au with a thickness of 50/200 nm was deposited in sequence. After the metallization, the metal lift-off process was carried out and the sample was cleaned in the acetone and methanol solutions for removing the photoresist residuals. The as-fabricated InAs NW photodetector was checked by a scanning electron microscope (SEM) (Hitachi S-4800, Tokyo, Japan) and an atomic force microscope (AFM) (D3100, Veeco, New York, United States). The surface chemical composition was characterized using an X-ray photoelectron spectroscope (XPS) (Thermo Escalab 250Xi, Waltham). The optoelectronic properties of the fabricated NW devices were characterized using a Lake Shore TTPX probe station together with a Keithley 4200A-SCS semiconductor parameter analyzer. The modulated continuous wave (CW) laser was used as pulsed incident signals, which was coupled to a multimode tapered optical fiber and guided to the tip as an optical probe. The pulse width and intensity could be precisely



tuned by the external modulator. The light spot shed on the sample was about 500  $\mu\text{m}^2$ . The dynamic response of the device was obtained by measuring the current at each moment under a given fixed voltage. Moreover, all tests were carried out at room temperature and atmospheric pressure.

The SEM image of the as-grown NW sample is shown in **Figure 1A**, and the nominal length of the InAs NWs is about 5  $\mu\text{m}$ . **Figure 1B** shows the three-dimensional schematic diagram of the device. **Figure 1C** presents a SEM image of an as-fabricated InAs NW photodetector device with the channel length about 1.8  $\mu\text{m}$  and the diameter about 35 nm. **Figure 1D** shows the AFM image of the InAs NW photodetector. The corresponding cross-sectional line profile records the height variation across the InAs NW. The maximum height (35.6 nm) marked with a pair of inverted triangles can be taken to represent the actual nanowire diameter.

## RESULTS AND DISCUSSION

As shown in **Figure 2A**, typical I-V curves were obtained when the NW device was exposed to laser illumination at different wavelengths (405, 650, and 940 nm), at a power density of 500 mW/cm<sup>2</sup>. Different from the conventional photoconductive photodetectors, our test results reveal that the photocurrent will decrease sharply as laser irradiation is shed on the NW device. It can be clearly found that the response of the nanowire detector to light becomes weaker as the wavelength of light irradiation increases. For the InAs NW photodetector with a physical size far smaller than the wavelength of incidence, refraction of photons may lead to a weak light absorption. This effect would get severer as the wavelength of incidence gets longer, which is one of the main factors for low photoresponse to the infrared light [39, 40]. In addition, the surface electron accumulation layer has a great influence on carrier transport, resulting in a lower detectivity in the

infrared regime as well [41–44]. Here, the  $I_{light}$  is defined as the photocurrent under the illuminated state. The  $I_{dark}$  is defined as the dark current, and the net photocurrent ( $I_{PC}$ ) is defined as  $I_{PC} = |I_{light} - I_{dark}|$ . **Figure 2B** shows the dark current to photocurrent ratio as a function of bias voltage at different wavelengths. Under different wavelengths of incidence, the maximum dark current to photocurrent ratios are ~130 (405 nm), ~25 (650 nm), and ~1.5 (940 nm).

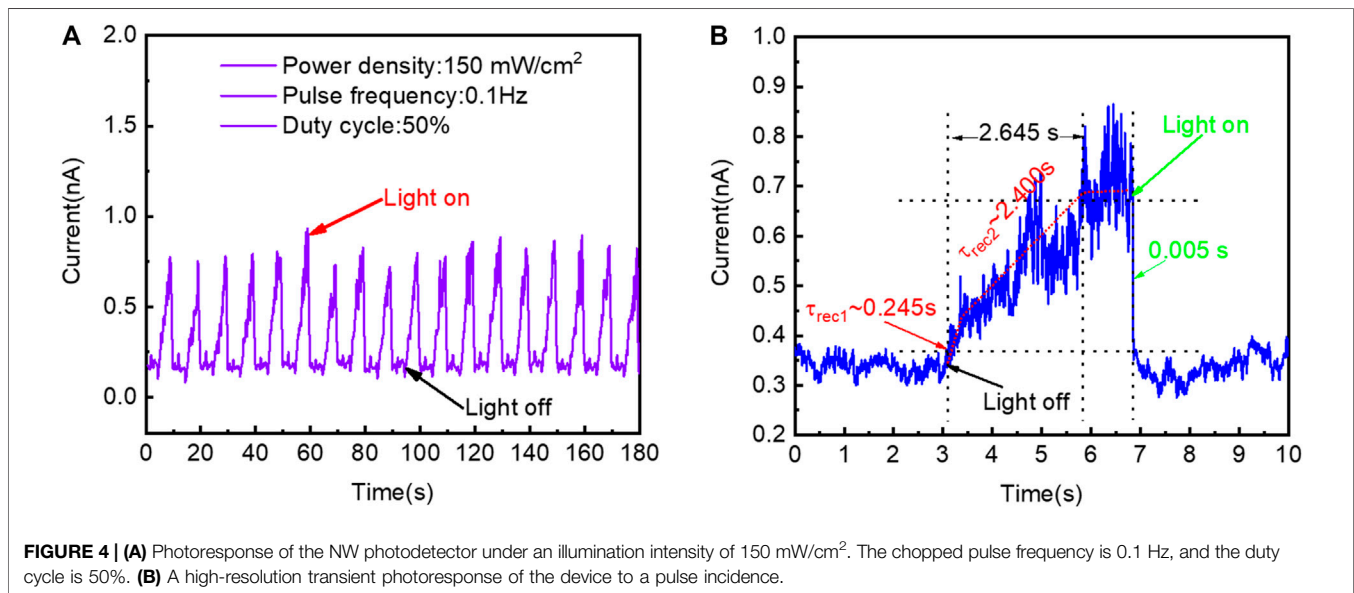
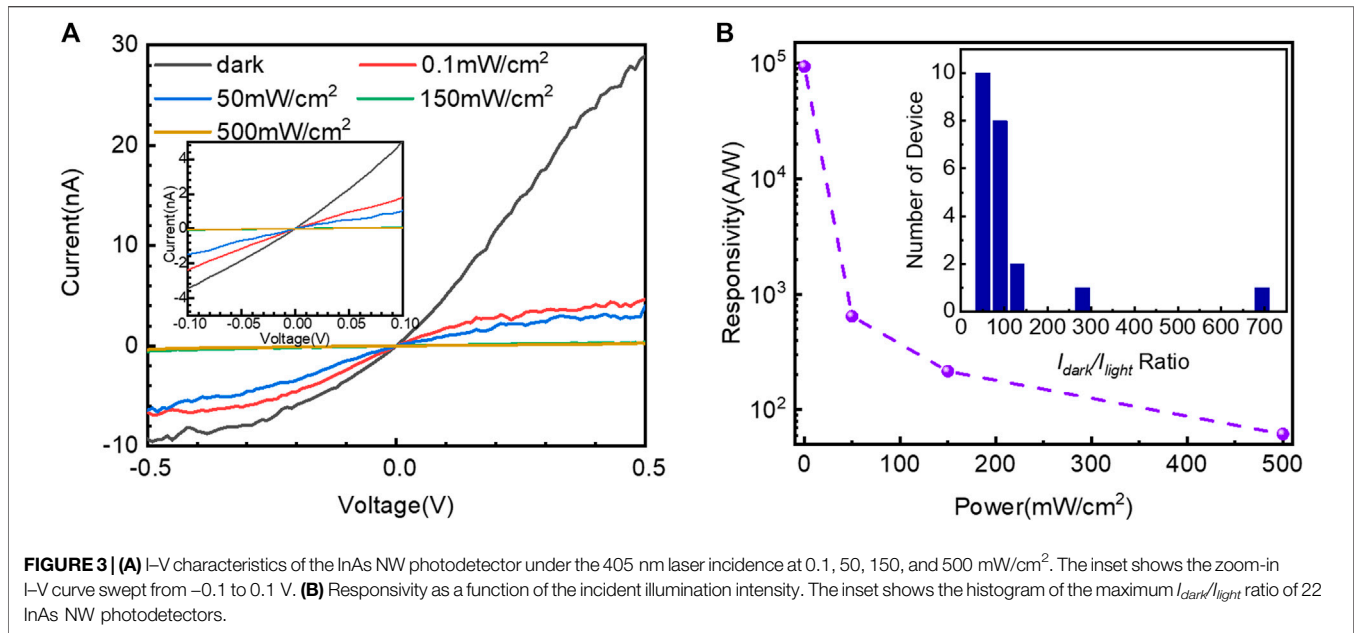
To further understand the photoresponse characteristic of these NW detectors, the dependence of device photocurrent to the laser irradiation intensities (0.1, 50, 150, and 500 mW/cm<sup>2</sup>) is investigated and depicted in **Figure 3A**. For a typical photodetector with a positive photoresponse, the photoconductive gain ( $G$ ), defined as the number of charges collected by the electrodes due to the excitation by one photon, can be expressed as [17]

$$G = \frac{I_{PC}}{e} \times \frac{h\nu}{P},$$

where  $h\nu$  is the energy of an incident photon,  $e$  is the electron charge, and  $P$  is the light power absorbed by the InAs NW. However, for the anomalous photoresponse in this work, the negative photoconductive gain is defined as the number of carriers absorbed by NWs per incident photon. In order to compare better with other NW detectors, which conventionally have a positive photoresponse, we chose to adopt this similar definition. The only difference is that the gain is negative in this case. Under the assumption that light incident on the channel is absorbed completely, a negative gain of  $2.8 \times 10^5$  is obtained at 0.2 V.

The photoresponsivity ( $R_\lambda$ ) is a very important parameter for a photodetector, which can be calculated as follows [28]:

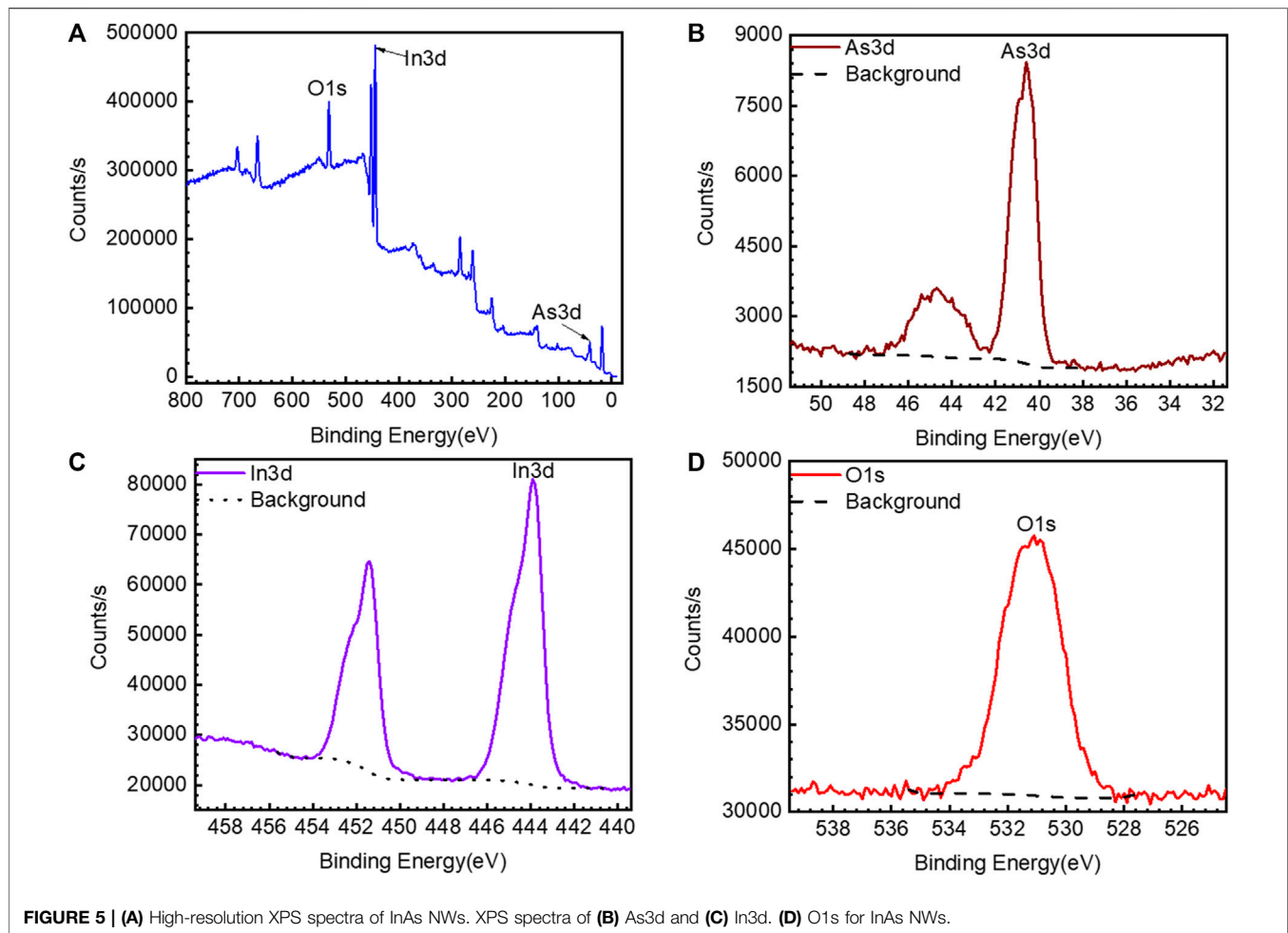
$$R_\lambda = \frac{|I_{PC}|}{P},$$



where  $I_{PC}$  is the net photocurrent and  $P$  is the light power absorbed by the NW. The responsivity of the device at a bias voltage of 0.5 V is shown in **Figure 3B**. The device exhibits a very large responsivity (closed to  $10^5$  A/W) when the light intensity is reduced to 0.1 mW/cm<sup>2</sup>, indicating a good sensitivity of the NW detector for weak signals. The inset shows the histogram distribution of the maximum  $I_{\text{dark}}/I_{\text{light}}$  ratio collected from 22 single InAs NW photodetectors. The devices all exhibit good negative photoelectric response, with the highest  $I_{\text{dark}}/I_{\text{light}}$  ratio of 700 being achieved.

The dynamic photoresponse is another important parameter to evaluate the performance of the detector. The

time-resolved photoresponse of NW photodetectors is shown in **Figure 4**. The frequency of the modulation signal is set as 0.1 Hz, while the duty cycle is 50% and the light intensity is 150 mW/cm<sup>2</sup>. The detector can work stably after dozens of complete cycles. The rise and decay time constants, defined as the time interval for the current rise from 10 to 90% of the peak value and vice versa, representing the response and recovery time, are found to be 0.005 and 2.645 s, respectively, indicating the fast response and the slow recovery of the device. Different from the positive photoresponse, although the negative photoresponse exhibits a relatively fast photocurrent



response process, the photocurrent recovery process is relatively slow. The slow recovery of photocurrent is believed to be caused by the increase in the dynamic relaxation time of carriers because of the traps in the light-induced gating layer. By fitting the light recovery current according to the following equation [32]:

$$I = I_0 \left[ 1 - \frac{A \exp(t_0 - t)}{\tau_{rec1}} - \frac{B \exp(t_0 - t)}{\tau_{rec2}} \right],$$

$\tau_{rec1}$  and  $\tau_{rec2}$  correspond to the lifetimes in the recombination processes. One is coming from the surface depletion region relaxation, and the other is a slow recovery process dominated by the trapping of carriers via defect states, which can be estimated to be about 0.245 s and 2.400 s, respectively, as shown in **Figure 4B**.

To further explain the NPC effect, the chemical composition of the nanowires was first tested and analyzed using the high-resolution XPS, as shown in **Figure 5**. From the spectra, three sharp peaks at 40.63, 443.99, and 531.14 eV can be observed, representing the As3d, In3d, and O1s peaks, respectively.

Furthermore, the In3d characteristic doublet peaks are shown in **Figure 5C**. The In3d 5/2 and In3d 3/2 binding energies appear at 443.9 and 451.4 eV, respectively. These observations have clearly shown the existence of the oxidation layer as the InAs NW exposed to the air. When there is no light, the free electrons in the NW core are driven by an external electric field to form a current, which is the so-called dark current. Due to the numerous defects, the Fermi level of the NW surface is pinned, leading to an energy bending in both conduction and valence bands. Acting as the PGL, the oxide layer would trap photogenerated carriers through the surface states, leading to a loss in the number of the carriers [29]. Additionally, it is worthy to note that surface scattering and recombination processes will also cause a degradation of the electron mobility close to the surface of the nanowire [45]. Meanwhile, as the incident power is very low, the photogenerated carriers would also recombine in the collection process, all contributing to a sharp decrease in the channel current. The NW size may play a role in the redistribution of carriers as well. [45, 46].

## CONCLUSION

To conclude, InAs NWs have been grown on *p*-type silicon (111) wafers by MBE, and high-performance MSM photodetectors have been demonstrated. A high responsivity of approximately  $10^5$  A/W, an NPC gain of over  $10^5$ , an  $I_{dark}/I_{light}$  ratio of more than 100, and a fast response time of less than 5 ms are obtained under normal temperature and pressure under 405 nm laser irradiation. Further analysis found that InAs nanowires are easily oxidized in the air, forming a gating layer, which can capture the photogenerated carriers in the nanowires. Moreover, this NW photodetector will pave a way to enable novel high-sensitivity broad-spectrum room-temperature detection.

## REFERENCES

- Dillen DC, Kim K, Liu E-S, and Tutuc E. Radial Modulation Doping in Core-Shell Nanowires. *Nat Nanotech* (2014) 9:116–20. doi:10.1038/nnano.2013.301
- Ju S, Facchetti A, Xuan Y, Liu J, Ishikawa F, Ye P, et al. Fabrication of Fully Transparent Nanowire Transistors for Transparent and Flexible Electronics. *Nat Nanotech* (2007) 2:378–84. doi:10.1038/nnano.2007.151
- Gudiksen MS, Lauhon LJ, Wang J, Smith DC, and Lieber CM. Growth of Nanowire Superlattice Structures for Nanoscale Photonics and Electronics. *Nature* (2002) 415(6872):617–20. doi:10.1038/415617a
- Ford AC, Ho JC, Chueh Y-L, Tseng Y-C, Fan Z, Guo J, et al. Diameter-Dependent Electron Mobility of InAs Nanowires. *Nano Lett* (2009) 9(1):360–5. doi:10.1021/nl803154m
- Kung S-C, van der Veer WE, Yang F, Donovan KC, and Penner RM. 20  $\mu$ s Photocurrent Response from Lithographically Patterned Nanocrystalline Cadmium Selenide Nanowires. *Nano Lett* (2010) 10(4):1481–5. doi:10.1021/nl100483v
- Takahashi T, Takei K, Adabi E, Fan Z, Niknejad AM, and Javey A. Parallel Array InAs Nanowire Transistors for Mechanically Bendable, Ultrahigh Frequency Electronics. *ACS Nano* (2010) 4(10):5855–60. doi:10.1021/nn1018329
- Takei K, Takahashi T, Ho JC, Ko H, Gillies AG, Leu PW, et al. Nanowire Active-Matrix Circuitry for Low-Voltage Macroscale Artificial Skin. *Nat Mater* (2010) 9(10):821–6. doi:10.1038/nmat2835
- Wallentin J, Anttu N, Asoli D, Huffman M, Aberg I, Magnusson MH, et al. InP Nanowire Array Solar Cells Achieving 13.8% Efficiency by Exceeding the Ray Optics Limit. *Science* (2013) 339(6123):1057–60. doi:10.1126/science.1230969
- Han N, Wang F, Hou JJ, Yip SP, Lin H, Xiu F, et al. Tunable Electronic Transport Properties of Metal-Cluster-Decorated III-V Nanowire Transistors. *Adv Mater* (2013) 25(32):4445–51. doi:10.1002/adma.201301362
- Saxena D, Mokkaapati S, Parkinson P, Jiang N, Gao Q, Tan HH, et al. Optically Pumped Room-Temperature GaAs Nanowire Lasers. *Nat Photon* (2013) 7(12):963–8. doi:10.1038/nphoton.2013.303
- Dayeh SA, Aplin DPR, Zhou X, Yu PKL, Yu ET, and Wang D. High Electron Mobility InAs Nanowire Field-Effect Transistors. *Small* (2007) 3(2):326–32. doi:10.1002/smll.200600379
- Dayeh SA. Electron Transport in Indium Arsenide Nanowires. *Semicond Sci Technol* (2010) 25(2):024004–24020. doi:10.1088/0268-1242/25/2/024004
- Joyce HJ, Gao Q, Wong-Leung J, Kim Y, Tan HH, and Jagadish C. Tailoring GaAs, InAs, and InGaAs Nanowires for Optoelectronic Device Applications. *IEEE J Select Top Quan Electron*. (2011) 17(4):766–78. doi:10.1109/JSTQE.2010.2077621
- Joyce HJ, Gao Q, Hoe Tan H, Jagadish C, Kim Y, Zou J, et al. III-V Semiconductor Nanowires for Optoelectronic Device Applications. *Prog Semicond* (2011) 35(2-3):23–75. doi:10.1016/j.pquantelec.2011.03.002
- Logeswaran VJ, Oh J, Nayak AP, Katzenmeyer AM, Gilchrist KH, Grego S, et al. A Perspective on Nanowire Photodetectors: Current Status, Future

## DATA AVAILABILITY STATEMENT

The original contributions presented in the study are included in the article/Supplementary Material, and further inquiries can be directed to the corresponding authors.

## AUTHOR CONTRIBUTIONS

YZ and DP conceived the idea and wrote part of the manuscript. XZ conducted the experiment and wrote the original version of the manuscript. XZ, YZ, and DP analyzed the results and prepared the figures. YZ proofread the manuscript. XY, JZ, and JL supervised the project. All authors have given approval to the final version of the manuscript.

- Challenges, and Opportunities. *IEEE J Sel Top Quan Electron* (2011) 17(4):1002–32. doi:10.1109/JSTQE.2010.2093508
- Das A, Ronen Y, Most Y, Oreg Y, Heiblum M, and Shtrikman H. Zero-bias Peaks and Splitting in an Al-InAs Nanowire Topological Superconductor as a Signature of Majorana Fermions. *Nat Phys* (2012) 8(12):887–95. doi:10.1038/NPHYS2479
- Miao J, Hu W, Guo N, Lu Z, Zou X, Liao L, et al. Single InAs Nanowire Room-Temperature Near-Infrared Photodetectors. *ACS Nano* (2014) 8(4):3628–35. doi:10.1021/nn500201g
- Rota MB, Ameruddin AS, Fonseka HA, Gao Q, Mura F, Polimeni A, et al. Bandgap Energy of Wurtzite InAs Nanowires. *Nano Lett* (2016) 16(8):5197–203. doi:10.1021/acs.nanolett.6b02205
- Lapierre RR, Robson M, Azizur-Rahman KM, and Kuyanov P. A Review of III-V Nanowire Infrared Photodetectors and Sensors. *J Phys D: Appl Phys* (2017) 50(12):123001. doi:10.1088/1361-6463/aa5ab3
- Dayeh SA, Soci C, Yu PKL, Yu ET, and Wang D. Influence of Surface States on the Extraction of Transport Parameters from InAs Nanowire Field Effect Transistors. *Appl Phys Lett* (2007) 90(16):162112. doi:10.1063/1.2728762
- Prins AD, Lewis MK, Bushell ZL, Sweeney SJ, Liu S, and Zhang Y-H. Evidence for a Defect Level above the Conduction Band Edge of InAs/InAsSb Type-II Superlattices for Applications in Efficient Infrared Photodetectors. *Appl Phys Lett* (2015) 106(17):171111. doi:10.1063/1.4919549
- Li B, Yan X, Zhang X, Luo Y, Lu Q, and Ren X. Controllable Photoresponse Behavior in a Single InAs Nanowire Phototransistor. *Appl Phys Lett* (2017) 111(11):113102. doi:10.1063/1.4990597
- Lynall D, Nair SV, Gutstein D, Shik A, Savelyev IG, Blumin M, et al. Surface State Dynamics Dictating Transport in InAs Nanowires. *Nano Lett* (2018) 18(2):1387–95. doi:10.1021/acs.nanolett.7b05106
- Shen L, Yip S, Lan C, Shu L, Li D, Zhou Z, et al. Enhanced Negative Photoconductivity in InAs Nanowire Phototransistors Surface-Modified with Molecular Monolayers. *Adv Mater Inter* (2018) 5(3):1701104. doi:10.1002/admi.201701104
- Zhang X, Yao X, Li Z, Zhou C, Yuan X, Tang Z, et al. Surface-States-Modulated High-Performance InAs Nanowire Phototransistor. *J Phys Chem Lett* (2020) 11(15):6413–9. doi:10.1021/acs.jpcclett.0c01879
- Halpern E, Elias G, Kretinin AV, Shtrikman H, and Rosenwaks Y. Direct Measurement of Surface States Density and Energy Distribution in Individual InAs Nanowires. *Appl Phys Lett* (2012) 100(26):262105. doi:10.1063/1.4731211
- Fang H, Hu W, Wang P, Guo N, Luo W, Zheng D, et al. Visible Light-Assisted High-Performance Mid-infrared Photodetectors Based on Single InAs Nanowire. *Nano Lett* (2016) 16(10):6416–24. doi:10.1021/acs.nanolett.6b02860
- Liu Z, Luo T, Liang B, Chen G, Yu G, Xie X, et al. High-detectivity InAs Nanowire Photodetectors with Spectral Response from Ultraviolet to Near-Infrared. *Nano Res* (2013) 6(11):775–83. doi:10.1007/s12274-013-0356-0
- Guo N, Hu W, Liao L, Yip S, Ho JC, Miao J, et al. Anomalous and Highly Efficient InAs Nanowire Phototransistors Based on Majority Carrier Transport

- at Room Temperature. *Adv Mater* (2014) 26(48):8203–9. doi:10.1002/adma.20147032910.1002/adma.201403664
30. Yang Y, Peng X, Kim H-S, Kim T, Jeon S, Kang HK, et al. Hot Carrier Trapping Induced Negative Photoconductance in InAs Nanowires toward Novel Nonvolatile Memory. *Nano Lett* (2015) 15(9):5875–82. doi:10.1021/acs.nanolett.5b01962
  31. Han Y, Zheng X, Fu M, Pan D, Li X, Guo Y, et al. Negative Photoconductivity of InAs Nanowires. *Phys Chem Chem Phys* (2016) 18(2):818–26. doi:10.1039/c5cp06139c
  32. Han Y, Fu M, Tang Z, Zheng X, Ji X, Wang X, et al. Switching from Negative to Positive Photoconductivity toward Intrinsic Photoelectric Response in InAs Nanowire. *ACS Appl Mater Inter* (2017) 9(3):2867–74. doi:10.1021/acsami.6b13775
  33. Zhou J, Gu Y, Hu Y, Mai W, Yeh P-H, Bao G, et al. Gigantic Enhancement in Response and Reset Time of ZnO UV Nanosensor by Utilizing Schottky Contact and Surface Functionalization. *Appl Phys Lett* (2009) 94(19):191103. doi:10.1063/1.3133358
  34. Chen M-W, Chen C-Y, Lien D-H, Ding Y, and He J-H. Photoconductive Enhancement of Single ZnO Nanowire through Localized Schottky Effects. *Opt Express* (2010) 18(14):14836–41. doi:10.1364/OE.18.014836
  35. Lind E, Persson AI, Samuelson L, and Wernersson L-E. Improved Subthreshold Slope in an InAs Nanowire Heterostructure Field-Effect Transistor. *Nano Lett* (2006) 6(9):1842–6. doi:10.1021/nl052468b
  36. Miao J, Hu W, Guo N, Lu Z, Liu X, Liao L, et al. High-Responsivity Graphene/InAs Nanowire Heterojunction Near-Infrared Photodetectors with Distinct Photocurrent On/Off Ratios. *Small* (2015) 11(8):936–42. doi:10.1002/sml.201402312
  37. Zhang X, Huang H, Yao X, Li Z, Zhou C, Zhang X, et al. Ultrasensitive Mid-wavelength Infrared Photodetection Based on a Single InAs Nanowire. *ACS Nano* (2019) 13:3492–9. doi:10.1021/acsnano.8b09649
  38. Pan D, Fu M, Yu X, Wang X, Zhu L, Nie S, et al. Controlled Synthesis of Phase-Pure InAs Nanowires on Si(111) by Diminishing the Diameter to 10 nm. *Nano Lett* (2014) 14(3):1214–20. doi:10.1021/nl4040847
  39. Hang Q, Wang F, Carpenter PD, Zemlyanov D, Zakharov D, Stach EA, et al. Role of Molecular Surface Passivation in Electrical Transport Properties of InAs Nanowires. *Nano Lett* (2008) 8(1):49–55. doi:10.1021/nl071888t
  40. Du J, Liang D, Tang H, and Gao XPA. InAs Nanowire Transistors as Gas Sensor and the Response Mechanism. *Nano Lett* (2009) 9(12):4348–51. doi:10.1021/nl902611f
  41. Olsson LÖ, Andersson CBM, Håkansson MC, Kanski J, Ilver L, and Karlsson UO. Charge Accumulation at InAs Surfaces. *Phys Rev Lett* (1996) 76(19):3626–9. doi:10.1103/PhysRevLett.76.3626
  42. Weber JR, Janotti A, and Van de Walle CG. Intrinsic and Extrinsic Causes of Electron Accumulation Layers on InAs Surfaces. *Appl Phys Lett* (2010) 97(19):192106. doi:10.1063/1.3518061
  43. Noguchi M, Hirakawa K, and Ikoma T. Intrinsic Electron Accumulation Layers on Reconstructed Clean InAs(100) Surfaces. *Phys Rev Lett* (1991) 66(17):2243–6. doi:10.1103/PhysRevLett.66.2243
  44. Ichikawa S, Sanada N, Mochizuki S, Esaki Y, Fukuda Y, Shimomura M, et al. Structure of anInAs(111)A-(2×2)Ssurface Studied by Scanning Tunneling Microscopy, Photoelectron Spectroscopy, and X-ray Photoelectron Diffraction. *Phys Rev B* (2000) 61(19):12982–7. doi:10.1103/PhysRevB.61.12982
  45. Li J, Yan X, Sun F, Zhang X, and Ren X. Anomalous Photoconductive Behavior of a Single InAs Nanowire Photodetector. *Appl Phys Lett* (2015) 107(26):263103. doi:10.1063/1.4938752
  46. He J, Chen K, Huang C, Wang X, He Y, and Dan Y. Explicit Gain Equations for Single Crystalline Photoconductors. *ACS Nano* (2020) 14:3405–13. doi:10.1021/acsnano.9b09406

**Conflict of Interest:** The authors declare that the research was conducted in the absence of any commercial or financial relationships that could be construed as a potential conflict of interest.

**Publisher's Note:** All claims expressed in this article are solely those of the authors and do not necessarily represent those of their affiliated organizations or those of the publisher, the editors, and the reviewers. Any product that may be evaluated in this article, or claim that may be made by its manufacturer, is not guaranteed or endorsed by the publisher.

Copyright © 2021 Zhang, Zhang, Pan, Yi, Zhao and Li. This is an open-access article distributed under the terms of the Creative Commons Attribution License (CC BY). The use, distribution or reproduction in other forums is permitted, provided the original author(s) and the copyright owner(s) are credited and that the original publication in this journal is cited, in accordance with accepted academic practice. No use, distribution or reproduction is permitted which does not comply with these terms.